

R-matrix analysis of reactions in the ${}^9\text{B}$ compound system

M. Paris,^{1,*} G. Hale,¹ A. Hayes-Sterbenz,¹ and G. Jungman¹

¹*T-2 Theoretical Division, Los Alamos Nuclear Laboratory,
MS B283, Los Alamos, New Mexico 87545, USA*

(Dated: April 29, 2021)

Recent activity in solving the ‘lithium problem’ in big bang nucleosynthesis has focused on the role that putative resonances may play in resonance-enhanced destruction of ${}^7\text{Li}$. Particular attention has been paid to the reactions involving the ${}^9\text{B}$ compound nuclear system, $\text{d}+{}^7\text{Be}\rightarrow{}^9\text{B}$. These reactions are analyzed via the multichannel, two-body unitary R -matrix method using code (EDA) developed by Hale and collaborators. We employ much of the known elastic and reaction data, in a four-channel treatment. The data include elastic ${}^3\text{He}+{}^6\text{Li}$ differential cross sections from 0.7 to 2.0 MeV, integrated reaction cross sections for energies from 0.7 to 5.0 MeV for ${}^6\text{Li}({}^3\text{He},\text{p}){}^8\text{Be}^*$ and from 0.4 to 5.0 MeV for the ${}^6\text{Li}({}^3\text{He},\text{d}){}^7\text{Be}$ reaction. Capture data have been added to an earlier analysis with integrated cross section measurements from 0.7 to 0.825 MeV for ${}^6\text{Li}({}^3\text{He},\gamma){}^9\text{B}$. The resulting resonance parameters are compared with tabulated values, and previously unidentified resonances are noted. Our results show that there are no near $\text{d}+{}^7\text{Be}$ threshold resonances with widths that are 10’s of keV and reduce the likelihood that a resonance-enhanced mass-7 destruction mechanism, as suggested in recently published work, can explain the ${}^7\text{Li}$ problem.

I. INTRODUCTION

Calculations of the abundance of ${}^7\text{Li}$ [1] overestimate the value extracted from observations of low-metallicity halo dwarf stars[2], where the stellar dynamics are supposed to be sufficiently understood to isolate the primordial ${}^7\text{Li}$ component. The discrepancy with this (and another[3]) observation by a factor of $2.2 \rightarrow 4.2$ corresponds to a deviation of $4.5\sigma \rightarrow 5.5\sigma$, a result that has only become more severe with time. It is essential to determine the nature of this discrepancy as big-bang nucleosynthesis (BBN) probes conditions of the very early universe and our understanding of physical laws relevant in an extreme environment.

Recent attention has focused on the role of reactions that destroy $A = 7$ nuclei at early times $\lesssim 1$ s in the big-bang environment[4, 5]. The authors of Ref.[4], citing the TUNL-Nuclear Data Group (NDG) evaluation tables[6], (See Table I.) conjecture that the putative $\frac{5}{2}^+$ resonance near 16.7 MeV may enhance the destruction of ${}^7\text{Be}$ through reactions like ${}^7\text{Be}(\text{d},\text{p})\alpha\alpha$ and ${}^7\text{Be}(\text{d},\gamma){}^9\text{B}$ if the resonance parameters are within given ranges. These studies employ the Wigner limit[10] to determine an upper bound on the contribution of resonances, particularly ${}^9\text{B}$, to a resonant enhancement in reactions that destroy mass-7 nuclides, ${}^7\text{Li}$ in particular. Because there is a

$E_x(\text{MeV} \pm \text{keV})$	$J^\pi; T$	$\Gamma_{\text{cm}}(\text{keV})$	Decay
16.024 ± 25	$T = (\frac{1}{2})$	180 ± 16	
16.71 ± 100	$(\frac{5}{2}^+); (\frac{1}{2})$		
17.076 ± 4	$\frac{1}{2}^-; \frac{3}{2}$	22 ± 5	$(\gamma, {}^3\text{He})$
17.190 ± 25		120 ± 40	p, d, ${}^3\text{He}$
17.54 ± 100	$(\frac{7}{2}^+); (\frac{1}{2})$		
17.637 ± 10		71 ± 8	p, d, ${}^3\text{He}$, α

TABLE I. The TUNL-NDG/ENSDF resonances in the ${}^9\text{B}$ compound nuclear system[6] for resonances that are low-lying with respect to the $\text{d}-{}^7\text{Be}$ threshold, which occurs at 16.4901 MeV.

paucity of data in the region near the $\text{d}+{}^7\text{Be}$ threshold where the assumed $\frac{5}{2}^+$ ${}^9\text{B}$ resonance inhabits, we wondered if the existing data may indicate the presence of such a resonance if a multichannel, unitary R -matrix evaluation is pursued.

Our motivation for the present study of the ${}^9\text{B}$ compound system is two-fold. The continuing light nuclear reaction program at Los Alamos National Laboratory, T-2 Theoretical Division provides light nuclear data for an array of end users, including the ENDF and ENSDF communities. Moreover, we are interested in updating the evaluation of the ${}^9\text{B}$ compound system to address the key question outlined above for BBN: does a resonance near the $\text{d}+{}^7\text{Be}$ threshold cause an increase in the destruction of mass-7 nuclides in the early universe and possibly explain the ${}^7\text{Li}$ overprediction problem?

* Corresponding author, electronic address:
mparis@lanl.gov

II. THE R-MATRIX FORMALISM AND EDA CODE

The R -matrix approach[7–9] is a unitary, multichannel parametrization that has proven useful for an array of nuclear reaction phenomenology, particularly for light nuclei[11]. We give only a brief description here and refer to the literature for a more complete description[12, 13].

We consider only $2 \rightarrow 2$ body scattering and reaction processes for light nuclear systems. Configuration space is partitioned into an interior, strongly interacting region and an exterior, Coulomb or non-polarizing interaction region by giving a channel radius, a_c for each two-body channel. The boundary of separation of these regions is the channel surface, $\mathcal{S} = \sum_c \mathcal{S}_c$.

The R matrix is computed as the projection on channel surface functions, $|c\rangle$ of the Green's function, $G_B = (H + \mathcal{L}_B - E)^{-1}$

$$R_{c'c} = (c'|H + \mathcal{L}_B - E)^{-1}|c\rangle = \sum_{\lambda} \frac{(c'|\lambda)(\lambda|c)}{E_{\lambda} - E}, \quad (1)$$

where \mathcal{L}_B is the Bloch operator, which accounts for the presence of a boundary condition, B on the channel surface. The Bloch operator ensures that the operator $H + \mathcal{L}_B$ is a compact, Hermitian operator having a real, discrete spectrum. The R -matrix parameters, E_{λ} and $\gamma_{\lambda c} = (c|\lambda)$ describe the spectrum and residues of the resolvent operator; they are treated as parameters adjusted to fit the observed data. Both hadronic and electromagnetic (*ie.* $\gamma+^9\text{B}$) channels can be handled in this approach. The transition matrix, \mathbf{T} the square of which gives the observables (cross section, etc.) of the theory, is given as

$$\mathbf{T} = \rho^{1/2} \mathbf{O}^{-1} \mathbf{R}_L \mathbf{O}^{-1} \rho^{1/2} - \mathbf{F} \mathbf{O}^{-1}, \quad (2)$$

where $\mathbf{R}_L = (\mathbf{R}^{-1} - \mathbf{L} + \mathbf{B})^{-1}$, $\mathbf{L} = \rho \mathbf{O}' \mathbf{O}^{-1}$, and $\mathbf{F} = \text{Im } \mathbf{O}$, where \mathbf{O} is the diagonal matrix of outgoing (Coulomb) wave functions in the exterior region.

The R -matrix approach is implemented in the EDA (Energy Dependent Analysis) code developed by Hale and collaborators[11]. The available two-body scattering and reaction data is described by minimization of the χ^2 function with respect to variation of the R -matrix parameters E_{λ} and $\gamma_{\lambda c}$.

III. ANALYSIS AND RESULTS

The R -matrix configuration, constructed for input into the EDA code, is given in terms of the included channel partitions (pairs), the LS terms for each partition, and the channel radii and boundary conditions, B_c for each channel.

We have included in the analysis the hadronic channels: $d+^7\text{Be}$ partition with threshold of 16.5 MeV with

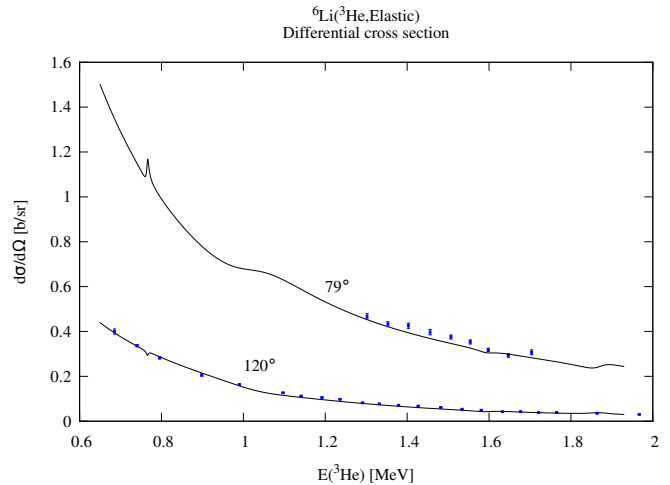


FIG. 1. Elastic scattering data from [15] plotted against the R -matrix fit (solid curve) for center-of-mass differential cross section vs. ^3He lab energy.

up to D -waves, $^3\text{He}+^6\text{Li}$ at 16.6 MeV up to P -waves, and $p+^8\text{Be}^*$ at 16.7 MeV up to P -waves. The channel radii were constrained to lie in the range between 5.5 fm and 7.5 fm for these. The electromagnetic $\gamma+^9\text{B}$ channels included were $E_1^{3/2}$, $M_1^{5/2}$, $M_1^{3/2}$, $M_1^{1/2}$, $E_1^{5/2}$, and $E_1^{1/2}$ with a channel radius of 50.0 fm.

The ^9B analysis is based upon data gathered from the literature and stored in the EXFOR/CSISRS database[14]. We include elastic differential cross section data for the $^6\text{Li}+^3\text{He}$ channel given in the range of ^3He lab energy, $1.30 \text{ MeV} < E(^3\text{He}) < 1.97 \text{ MeV}$ [15]; integrated cross section data for $^6\text{Li}(^3\text{He}, p)^8\text{Be}^*$ [16] where the final state channel is an average of the excited-states of the quasi-two-body final state of $p+^8\text{Be}^*$ given, in the range $0.66 \text{ MeV} < E(^3\text{He}) < 5.00 \text{ MeV}$; integrated cross section for the $^6\text{Li}(^3\text{He}, d)^7\text{Be}$ [17] in the range $0.42 \text{ MeV} < E(^3\text{He}) < 4.94 \text{ MeV}$; and capture data from the $^6\text{Li}+^3\text{He}$ initial state in the energy range $0.7 \text{ MeV} < E(^3\text{He}) < 0.825 \text{ MeV}$ [18].

Using about 40 parameters, the results of the χ^2 minimization result in a T matrix which gives the solid curves appearing in Figs.1–4, plotted along with the data obtained from references cited in the paragraphs above. The fit quality is fair with χ^2/datum of 1.91, 0.55, 2.38, and 0.37 for Figs.1–4, respectively. The fit to the capture data, Fig.4 has been folded with a Gaussian acceptance function whose width is 5 keV to match the quoted energy resolution in Ref.[18].

The present R -matrix parametrization gives a resonance structure as presented in Table II. The resonance poles of the T matrix are determined by diagonalization of the complex “energy-level” matrix

$$\mathcal{E}_{\lambda'\lambda} = E_{\lambda} \delta_{\lambda'\lambda} - \sum_c \gamma_{c\lambda'} [L_c(E) - B_c] \gamma_{c\lambda}, \quad (3)$$

$E_x(\text{MeV})$	J^π	$\Gamma(\text{keV})$	$\text{Re}E_0(\text{MeV})$	$\text{Im}E_0(\text{keV})$	$E(^3\text{He})(\text{MeV})$	Strength	
16.4754	$1/2^-$	768.46	-0.1369	-384.2	-0.2054	0.06	weak
17.1132	$1/2^-$	0.14	0.5109	-0.07	0.7664	1.00	strong
17.2012	$5/2^-$	871.63	0.5989	-435.8	0.8984	0.40	weak
17.2809	$3/2^-$	147.78	0.6785	-73.9	1.0178	0.77	strong
17.6754	$5/2^+$	33.33	1.0631	-16.7	1.5947	0.98	strong
17.8462	$7/2^+$	2036.21	1.2339	-1018.1	1.8509	0.15	weak
17.8577	$3/2^-$	42.52	1.2454	-21.3	1.8681	0.97	strong
18.0582	$3/2^+$	767.11	1.4459	-383.6	2.1689	0.54	weak
18.4229	$1/2^+$	5446.32	1.8206	-2723.2	2.7309	0.03	weak
18.6872	$1/2^-$	10278.41	2.0749	-5139.2	3.1124	0.15	weak
19.6192	$3/2^-$	1478.22	3.0069	-739.1	4.5104	0.52	weak

TABLE II. The resonance structure determined in the present 4-channel fit to data as described in the text. The table displays the pole location along with J^π and pole-strength information, as described in the text.

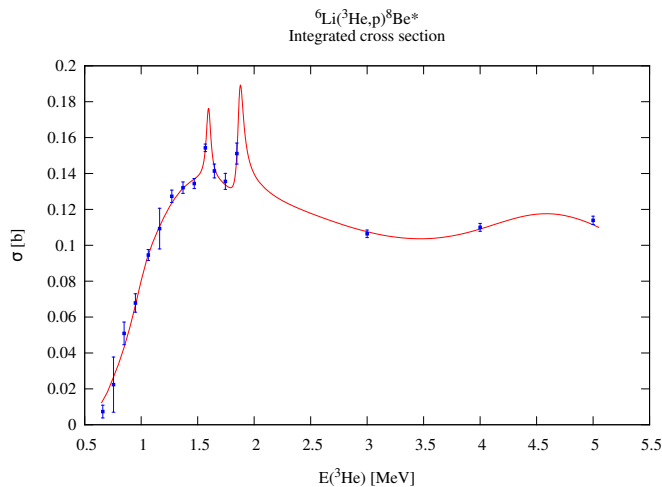


FIG. 2. Reaction data from [16], integrated cross section vs. ^3He lab energy.

where $L_c(E) = r_c(\partial\mathcal{O}/\partial r_c)\mathcal{O}^{-1}|_{r_c=a_c}$, \mathcal{O} is the outgoing Coulomb wave function, and B_c is the boundary condition given at the channel radius, a_c . Details are given in Ref.[19].

The first column of Table II gives the real part of the pole position, $E_0 = E_r - i\Gamma/2$, where E_0 is one of the eigenvalues of the energy-level matrix, Eq.(3) relative the ground state of ^9B . The spin-parity is given in the second column. The width Γ is the center-of-mass width in keV. The following column restates the real part of the resonance pole position relative the $^3\text{He}+^6\text{Li}$ threshold in the center-of-mass. The column labeled $E(^3\text{He})$ is the corresponding lab energy. The ‘Strength’ function is the ratio of the sum of the channel widths (defined in Ref.[19]) divided by the total width, $\Gamma^{-1}\sum_c\Gamma_c$. Resonances labeled ‘strong’ are clearly seen in at least one of the figures.

The resonance structure shown in Table II differs significantly from that in Table I. Possible reasons for the discrepancy include the fact that the current analysis is the first, to our knowledge, that includes much of the

available data in the region below $E(^3\text{He}) < 3.0$ MeV in a two-body unitary analysis. Several deductions about the resonance structure in the TUNL/ENSDF tables rely on associated production of ^9B experiments and single-level R -matrix parametrizations[6]. While more data, particularly polarization observables, would constrain the current fit with greater confidence, the present analysis appears to be the most comprehensive available that accounts for the available data in a two-body unitary way.

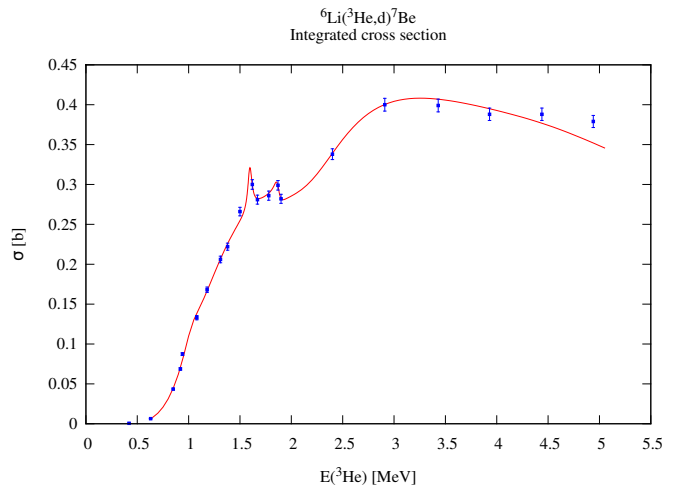


FIG. 3. Reaction data from [17], integrated cross section vs. ^3He lab energy.

Returning the problem of the overprediction of ^7Li in current treatments of BBN, we see that the requirements for a near-threshold resonance of Refs.[4] and [5] are difficult to arrange given the resonance structure of Table II. Both of these works require a narrow resonance, a few 10^3 ’s of keV in width with a 100 keV of the $^3\text{He}+^6\text{Li}$ (that is, 200 keV within the $d+^7\text{Be}$) threshold in order to explain the overproduction of ^7Li in BBN reaction network codes[1].

The current study does not conclusively eliminate the possibility of the mechanism of resonant enhancement

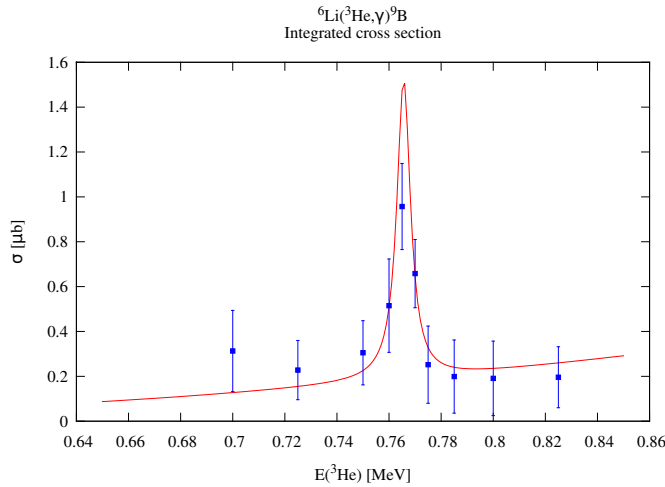


FIG. 4. Capture data from [18], integrated cross section vs. ^3He lab energy.

of mass-7 destruction. The ^9B compound system was identified originally by Cyburt and Pospelov[4] as playing a potential role in the destruction of ^7Be precisely because there isn't much data in the region near the $d+^7\text{Be}$ threshold. Our analysis is performed on essentially the same data that the existent TUNL-NDG analyses[6] were performed, with the smallest energy probed about 400–500 keV above the $^3\text{He}+^6\text{Li}$ threshold. It might, therefore, be suspected that the present data set would give no indication of such a low-lying resonance. Our experience with R matrix analysis indicates, however, that a resonance of 10's of keV in width would likely – but not certainly – have contributions ‘in the tail’ to the observables considered in the present study, particularly in the

$^6\text{Li}(^3\text{He}, d)^7\text{Be}$ integrated cross section of Fig.3.

IV. SUMMARY, FINDINGS AND FUTURE WORK

We've studied a possible resonant enhancement of the destruction of mass-7 (^7Be , in particular) in BBN scenarios. The near threshold, narrow state anticipated in Refs.[4] and [5] appear not to be supported by our multichannel, two-body unitary R -matrix analysis. We have reviewed the R -matrix method implemented in the Los Alamos reaction code for light nuclei, EDA and have discussed the included data from four channels: elastic $^3\text{He}+^6\text{Li}$, $^6\text{Li}(^3\text{He}, p)^8\text{Be}^*$, $^6\text{Li}(^3\text{He}, d)^7\text{Be}$ and $^6\text{Li}(^3\text{He}, \gamma)^9\text{B}$.

Our analysis determines a resonance structure significantly different from that published in the TUNL-NDG/ENSDF compilation[6], as can be seen by comparing the results from the present analysis in Table II with the table, Table I for the TUNL-NDG/ENSDF analysis. Our immediate objective is to incorporate the $^8\text{Be}^*$ final states for each excited state (rather than averaging their contribution as we have done in the present analysis). This will allow the extension of the present analysis to higher energies and the incorporation of polarization data[20, 21] that we have neglected.

Our findings for the role of a putative resonance in ^9B near the $d+^7\text{Be}$ threshold as envisioned in Refs.[4] and [5] is that their particular mechanism of resonant enhancement of mass-7 destruction is an unlikely explanation to the ^7Li problem in BBN, though low-energy data would allow a more conclusive statement of this finding or its converse.

This work was carried out under the auspices of the National Nuclear Security Administration.

-
- [1] B. D. Fields, *Ann. Rev. Nucl. Part. Sci.* **61**, 47 (2011), and references therein.
 - [2] F. Spite and M. Spite, *Astron. Astrophys.* **115**, 357 (1982).
 - [3] González Hernández, *et al.* *Astron. Astrophys.* **505**, L13-L16 (2009).
 - [4] R. H. Cyburt and M. Pospelov, *Int. J. Mod. Phys. E* **21**, 1250004 (2012).
 - [5] N. Chakraborty, B. D. Fields and K. A. Olive, *Phys. Rev. D* **83**, 063006 (2011)
 - [6] D. R. Tilley, J. H. Kelley, J. L. Godwin, D. J. Millener, J. E. Purcell, C. G. Sheu and H. R. Weller, *Nucl. Phys. A* **745**, 155 (2004).
 - [7] P. L. Kapur and R. Peierls *Proc. R. Soc. Lond. A* **166** 277-295 (1938).
 - [8] E. P. Wigner, *Phys. Rev.* **70**, 15 (1946).
 - [9] E. P. Wigner and L. Eisenbud, *Phys. Rev.* **72**, 29 (1947).
 - [10] Teichmann, T. and Wigner, E. P. *Phys. Rev.* **87**, 123–135 (1952).
 - [11] G. M. Hale, *Nuc. Data Sheets*, **109**, 2812-2816 (2008).
 - [12] A. M. Lane and R. G. Thomas, *Rev. Mod. Phys.* **30**, 257 (1958).
 - [13] A. M. Lane and D. Robson, *Phys. Rev.* **151**, 774 (1966).
 - [14] <http://www-nds.iaea.org/exfor/exfor.htm>
 - [15] S. Buzhin'ski, *et al.*, *Izv. Rossiiskoi Akademii Nauk, Ser.Fiz.* **43**, 158 (1979).
 - [16] A. J. Elwyn, R. E. Holland, C. N. Davids, J. E. Monahan, F. P. Mooring and W. Ray, *Phys. Rev. C* **22**, 1406 (1980).
 - [17] Cited in Holland *et al.*, *IEEE Trans. Nucl. Sci.* **NS-28**, 1344 (1981).
 - [18] M. R. Aleksic and R. V. Popic, *Fizika* **10**, 273–278 (1978).
 - [19] G. M. Hale, R. E. Brown and N. Jarmie, *Phys. Rev. Lett.* **59**, 763 (1987).
 - [20] Simons, *Bull. Am. Phys. Soc.*, **11**, 301 (1966).
 - [21] Simons, in *Polarization Phenomena in Nuclear Reactions*, Madison (1970), p. 597 (1971).